

Elsevier Editorial System(tm) for Composites Part A  
Manuscript Draft

Manuscript Number:

Title: Reference and computational framework for the flow front shape evaluation in LCM processes

Article Type: Research Paper

Keywords: homotopy  
homotopy maps  
configuration spaces  
on-line control systems

Corresponding Author: Mr Nicolas Montes, Ph.D Student

Corresponding Author's Institution: University CEU Cardenal Herrera

First Author: Nicolas Montes, Ph.D Student

Order of Authors: Nicolas Montes, Ph.D Student; Fernando Sanchez, PhD professor; Antonio Falco, PhD professor

Abstract: This paper presents a mathematical definition of the idealized flow fronts shapes for LCM processes. This definition is based on the continuous deformation of the naturally produced shapes of the front, radial to the injector, and the deformation needed to prevent dry areas, radial to the vent. Both definitions are useful as demonstrated in other studies, but they are each the opposite of the other.

To compare the homotopic map with the advance front shapes in a real or simulated process efficiently, the concept of configuration space, [24] is used. This gives a new configuration space that has been named Flow Pattern Homotopy Space (FPHS). In this paper we propose two applications as examples. In the first one, this space has been used to modify the PPI numerical indices proposed in [26] and [27] and the second one to use it for real time control systems.

Suggested Reviewers: Nuno Correia  
[Nuno.Correia@inegi.up.pt](mailto:Nuno.Correia@inegi.up.pt)  
has an impact papers in control systems

Edu Ruiz  
[edu.ruiz@polymtl.ca](mailto:edu.ruiz@polymtl.ca)

S.G. Advani  
[advani@udel.edu](mailto:advani@udel.edu)

Francisco Chinesta  
[Francisco.Chinesta@ec-nantes.fr](mailto:Francisco.Chinesta@ec-nantes.fr)



**Composites part A: Applied Science and Manufacturing**

# Reference and computational framework for the flow front shape evaluation in LCM processes

N. Montes \*, F. Sánchez, A. Falco

Universidad CEU Cardenal Herrera  
C / San Bartolomé 55, E-46 115, Alfara del Patriarca, Valencia (Spain)

\* Corresponding author email: nimonsan@uch.ceu.es

**Abstract:** This paper presents a mathematical definition of the idealized flow fronts shapes for LCM processes. This definition is based on the continuous deformation of the naturally produced shapes of the front, radial to the injector, and the deformation needed to prevent dry areas, radial to the vent. Both criteria have been extensively and separately used in other studies for optimization algorithms, on-line control and PPI (Process Performance Index), and they each deal with an ideal advance front shape. Both definitions of optimum front shapes are useful as demonstrated in other studies, but they cannot represent the optimum front shape because they are each the opposite of the other. In fact, when the advance front is near the injector, the latter should be radial to it but, when near the vent, the advance front must be radial to the vent and not to the injector. This behavior is known mathematically as homotopy. So, via this definition we can continuously define what the optimum advance front shapes should be like in LCM processes, resulting in a map with the ideal front shapes - a homotopy map. To compare the homotopic map with the advance front shapes in a real or simulated process efficiently, the concept introduced in our earlier work, [24], is going to be used. In this paper, the concept of configuration space was put forward as the computational context for LCM processes. This concept attempts to represent the Cartesian space in another alternative space made with the process's variables. In [24], a generic template space consisting of one fixed variable and another free one was proposed. The fixed variable was the angle defined between the point of interest and each node that formed the mesh. The Euclidean or geodesic distance was proposed as a free variable, and the normalized time at which the flow reached each node. In the present work, the normalized time at which the flow should arrive is to be selected as a free variable, obtained from the *homotopy map*. This gives a new configuration space that has been named *Flow Pattern Homotopy Space (FPHS)*. In this space, if the real advance front is the one obtained in the homotopy space, this will be seen as a straight line. In this paper we propose two applications as examples of application for this new computational space. In the first one, this space has been used to modify the PPI numerical indices (Process Performance Index) proposed in [26] and [27]. It allows to generalize the proposed PPI for whatever LCM process without increasing the computational costs. As demonstrated in this article, as the resolution of the distribution channels computed in our previous works, [24], [25], increases, the indicator of flow front idealness decreases. As a second example of application, it is proposed to use these spaces for real time control systems. As shown in this article, the decision-making is done almost intuitively by the controller.

## 1 Introduction

LCM (Liquid Composite Molding) processes can be classified in many ways. One of the most common ways is to classify them according to the pressure gradient needed to move the flow. Following this premise, processes such as RTM (Resin Transfer Molding) can be classified as positive gradient processes, and VARTM (Vacuum Assisted Resin Transfer Molding), VI (Vacuum Infusion) or RTM-Light processes as negative pressure gradient processes. Another way of classifying them may be by the characteristics of the countermold. In this sense we can

consider RTM processes as rigid counter-mold processes whereas VARTM, VI or counter-mold RTM-light type processes can be seen as semi-rigid or flexible, where for VI processes the counter-mold is a plastic bag. Another possible classification that can be made for LCM processes is according to the resin transfer system and air extraction. Thus, whereas in the RTM process the resin transfer system and air extraction are discrete gates, in VARTM, VI or RTM-light processes these systems may be distribution channels whose shape may be variable. There is also a differentiation between the VARTM and VI processes worth noting. Whereas in VARTM processes the most common method for filling is to place a distribution channel on the mold's perimeter, creating the vacuum at a point in the interior, in VI processes the opposite is the case - the vacuum is placed on the perimeter and the flow is introduced through a distribution channel located inside the mold. Table 1 shows the different ways of classifying LCM processes.

VARIABLES				
PROCESS	Pressure differential	resin transfer	air extraction	counter-mold
<b>RTM</b>	pressure-atmosphere	Discrete port	Discrete gate	Rigid
<b>RTM-Light</b>	atmosphere-vacuum	Perimeter	Discrete gate	Semi-rigid
<b>VARTM</b>	atmosphere-vacuum	Perimeter or surface	Discrete gate or surface	Flexible disposable
<b>VI</b>	atmosphere-vacuum	Perimeter and/or discrete gate	perimeter	Disposable vacuum bag

Table 1 Characterization of the different LCM processes.

## 1.1 Optimization and on-line control algorithms

On designing any of these processes, the problem must first be defined, as well as the specifications that the item to be designed must meet. From this information, a series of solutions are drawn up using a summarizing process basically backed up by experience, the designer's knowledge and simulation tools. Any possibly viable solutions are then analyzed to verify their effectiveness. This whole process is not linear; rather it is an iterative task that enables us to improve the proposed solution until the final design is reached. This iterative task is known as optimization, and the iterative processes are known as optimization algorithms. Traditionally, this work - both the summarizing and evaluation work - has been carried out with methods based on empirical knowledge. Furthermore, as the number of possible combinations in design as regards choice of materials, choice of the location of transfer systems and air extraction, etc., is practically unlimited, characterization by experimentation is very costly and in some cases impossible. This reliance on experimentation prevents wider use of the compounds in most common applications. For this reason, many research studies are based on the use of mathematical models and numerical methods such as the FEM to predict and simulate their behavior in order to create a good tool to help in this complicated design process. The design variables (process inputs), such as permeability, viscosity, injection pressure, flow rate, location of gates, etc., are introduced into the simulation algorithms so that objective functions can be calculated for the optimization model.

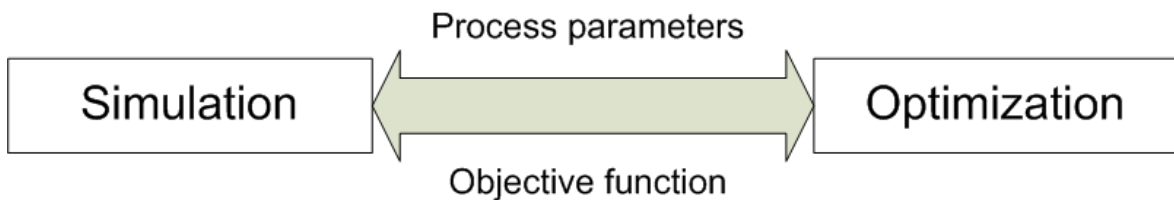


Fig 1 Optimization of LCM processes based on simulation.

One of the most crucial tasks in designing any LCM process is the location of the resin transfer system and air extraction. A bad choice can lead to bad filling, dry areas, bubbles, excessive filling time, bleeding, etc. We can find a great amount of reference material on optimization tools for rigid counter-mold processes ([1]-[10]) where the aim is to find the best location for the discrete gates. On the other hand, there are not many contributions that provide solutions as to the location of the transference systems and air extraction in semi-rigid or flexible counter-mold processes ([11] and [12]), mainly due to the complexity involved in having to optimize distribution channels.

The dependence of the results on experiments in optimization algorithms means that, when it comes to making the piece, imperfections appear in the models obtained, as well as new discrepancies between the assumptions made in the optimization and the reality of the process. One of the most common discrepancies is associated with the differences in permeability. When the preform is placed in the mold, the operator handling it may make mistakes in placing it. One of the most common mistakes is failing to adjust the preform precisely within the limits of the mold. On filling, this creates what is known as "*race tracking*", a zone of high permeability. In semi-rigid or flexible counter-mold processes, the problem of lack of homogeneity in permeability is increased since the differences in thickness produced by the flexibility of the counter-mold result in different permeability zones that are practically unpredictable. Therefore, along with the proliferation of optimization algorithms, researchers have worked on the on-line control of LCM processes. On-line control aims to achieve optimum filling during the filling process, whereas optimization is an off-line process that attempts to get the same result by considering certain known process variables that are invariable during the process. Therefore, on-line control of a certain process may be considered as an off-line optimization method, but one where restrictions on the control algorithms' calculation time are far more crucial since they directly affect the system's ability to react. In other studies we can find a great many contributions that attempt to solve online control of LCM processes ([13]-[22]).

## 1.2 The computational costs problem

One of the main problems associated with optimization algorithms and on-line control algorithms is the computation time. In optimization algorithms, this can be considered less essential because it is a task that is performed off-line. However, the algorithms put forward in other studies, focusing on optimizing inlets/outlets, are too lengthy. This is because in general genetic algorithms are being used coupled with simulation by finite elements ([2]-[12]). In all these works there has been a significant attempt to reduce the algorithm computation times, firstly by reducing the number of simulations needed (in [3] only 1% of the total are needed) and also by replacing the simulation by approximations with a lower computational workload (in [5] the simulation is replaced with a properly trained neural network that can take on the role of simulation). In [6] and [12], the simulation is replaced with what is known as "*mesh*

1  
2  
3  
4  
5  
6  
7  
8  
9  
10  
11  
12  
13  
14  
distance based approach." In this case, the distance measured on the mesh is considered as an approximation of the time obtained from the simulation. Much work has also been done on the use of genetic algorithms. In [4], the use of genetic algorithms is compared with brute force methods and those based on gradients such as the quasi-Newton method. In conclusion, the search method based on brute force alone is efficient for a small number of variables. Gradient-based methods are more efficient than genetic ones when there are many parameters, but if one or more of them are discrete, such as injectors and vents, it is no longer as efficient as the genetic algorithm. In [4], it is recommended that a combination of both be used. This hybrid optimization algorithm is used in [9]. Another modification proposed for the genetic algorithm is suggested in [7], where the search is based on branching and bounding. In [10], the use of a map-based exhaustive search is introduced into the branch and bound.

15  
16  
17  
18  
19  
20  
All of the work carried out over the years has managed to reduce the calculation time, from the work presented in [3] for rigid counter-mold processes that required 75 hours for a model with 448 finite elements to the one carried out in [12] for flexible counter-mold processes that needs 17 minutes to find the optimum solution for a simple geometric shape like a rectangle made up of 600 finite elements.

21  
22  
23  
24  
25  
26  
27  
28  
29  
30  
In the on-line control systems proposed in past studies, something similar occurs since they necessarily require prediction of flow behavior, given an instant of time for the control system [13] - [22]. This prediction necessarily requires simulation by finite elements, which has a high computational workload for it to be introduced in on-line processes where the calculation time mitigates the system's response time. Because of this, as in optimization algorithms, there are several papers that talk about how to achieve a simulation that is more efficient in computation time. These fast simulators are known as "*proxy simulators*." As with optimization algorithms, work has also been done to reduce the simulation computation time, where the lines of action are similar. In [15], [16], and [17] the use of neural networks is put forward to replace the simulation.

35  
36     **3.3 The benchmark definition problem.**

37  
38  
39 One of the most important tasks that determine the outcome obtained, both in optimization  
40 algorithms and in the on-line control of LCM processes, is the definition of what the optimum  
41 filling is, this being an objective function of the optimization algorithms and a benchmark for  
42 online control systems. In general, the goal in LCM processes is to completely saturate the  
43 preform with resin in the shortest possible time, before the reagent that activates the curing  
44 reaches the threshold where the resin viscosity increases abruptly. Thus, since the percentage  
45 of concentration of the catalyst with the resin is the same, the mold's curing begins at different  
46 moments in time. This is because the moment in time when the resin begins to gel depends on  
47 the percentage of catalyst and on the time this has been mixed with the resin. Thus, the  
48 gelification reaction can be modeled according to the time and the temperature recordings.  
49 This temperature gradient throughout the gelification process causes thermomechanical strain,  
50 leading the final piece to be lacking the desired properties.

51  
52  
53  
54 While there is unanimity in previous works in defining what the optimum curing phase should  
55 be like, the same cannot be said for which shapes the ideal advance front should be during the  
56 filling phase. On the one hand, some studies use the natural optimum advance front shape, i.e.  
57 radial and equidistant from the point of injection. However, other studies define and use the  
58  
59  
60  
61  
62  
63  
64  
65

optimum advance front shape as circular and equidistant but in this case to the vent. The third possibility used in other studies is to consider the optimum advance front shapes to be those obtained from simulation. This option is not correct since only in simple cases are ideal fillings carried out from a simulation. In Fig. 2 a comparison is shown of the ideal front shapes for each case, for a square mold.

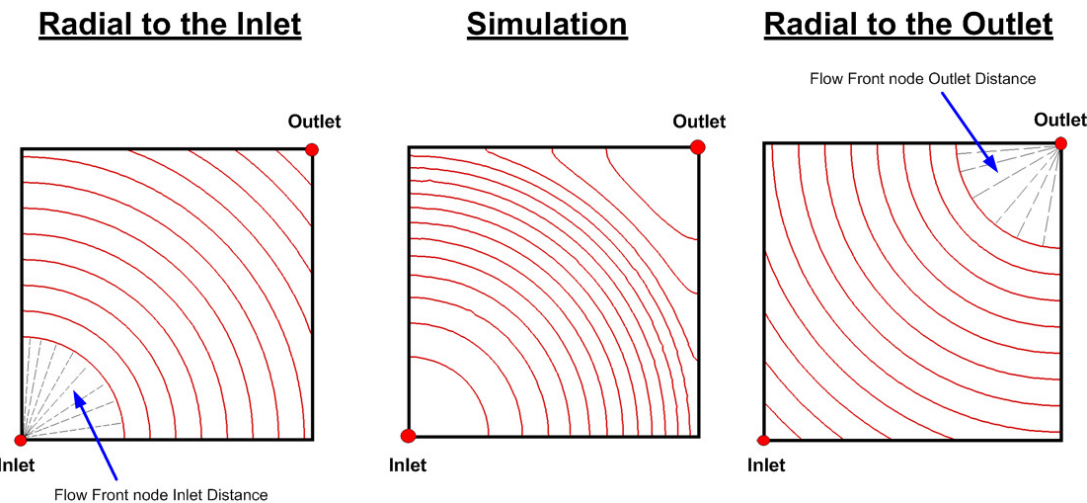


Fig. 2 Optimum shapes for the optimum front. Equal distance to the injector, left, equal distance to vent, right, and via simulation, middle.

In the optimization algorithms, there are studies using simulation that do not condition the advance front to any specific shape but which are based on a search within a simulation by finite elements ([3] and [11]). Although these studies do not directly condition the shape of the advance front, this should be the one obtained from the simulation in order for it to comply with the result obtained in the optimization process. In these studies, the objective function quantifies the dry areas produced where the best inlet/outlet distribution is the one that minimizes them. In [2] the optimum flow front pattern is defined as one that is uniform, in order to avoid uneven advances and to thereby minimize the production of dry areas. In [5], the uniform advance front that minimizes the production of dry areas is defined as one that is equally distant in all its nodes from the vent, at all instants of time. This criterion of optimal front shape has been established as the ideal advance front shape for measuring how optimum the manufacturing process of a particular piece has been. Thus, in [26] and [27] two numerical indices are proposed, known as PPI's (*Process Performance Index*), where one of the measurements of how good the filling process has been is the equidistance of the advancing front from the vent. In [26], the total filling time is also used whereas in [27] the index proposed in [26] is extended, including a numerical indicator to determine how ideal the curing process is. In this case the dispersion of the incubation time is used as a criterion.

On the other hand, other papers on optimization of inlets/outlets work with the natural ideal behavior of flow on an isotropic model, that is to say, radial to the injector. This flow behavior model is used in [4], [6], [7], [8], [9] and [10] as a criterion to classify the points farthest from the injector as possible places to locate the vent. In these studies, the optimization algorithm seeks the optimum position for the injector so that the filling phase is carried out in the shortest possible time. In [12], the same criterion is used as in [4], [6], [7], [8], [9] and [10], with the exception that it is applied to flexible countermold processes, where the injector does not necessarily have to be a point.

In the case of control algorithms, the definition of optimum front shape is more crucial than in optimization algorithms since the controller intends to force the shape of the front to become the one defined as the benchmark. In the great majority of studies put forward, simple geometries are usually used such as a rectangle ([13], [14], [15], [16], [17], [19], [21] and [22]) or a square ([20]) to test the algorithms. In these algorithms, there are different criteria to define what the optimum front shapes should be. In [13], [14], [15] and [18], the shape of the optimum advance front is the one obtained from a simulation. In [19] and [21], they test control algorithms in VARTM processes. In this case, the injector is a distribution channel placed to one side while the vent is a distribution channel on the other side. In this simple case, the shape of the ideal flow front must be equidistant from the injector, and inherently so to the vent. In [16], [17] and [22] they test both criteria - homogeneity of the injector/vent in a rectangle and simulation in defining the optimum advance front shape. In [20] a simple case is also analyzed, in this case a square, for infusion processes. An injector is placed in every corner of the square whereas the vent is placed at the square's center. In [20], the aim of the control system is to get the advance front to be equally distant from the vent at all times. As a summary, in Fig. 3 there is a table of the different references taken into account in other studies.

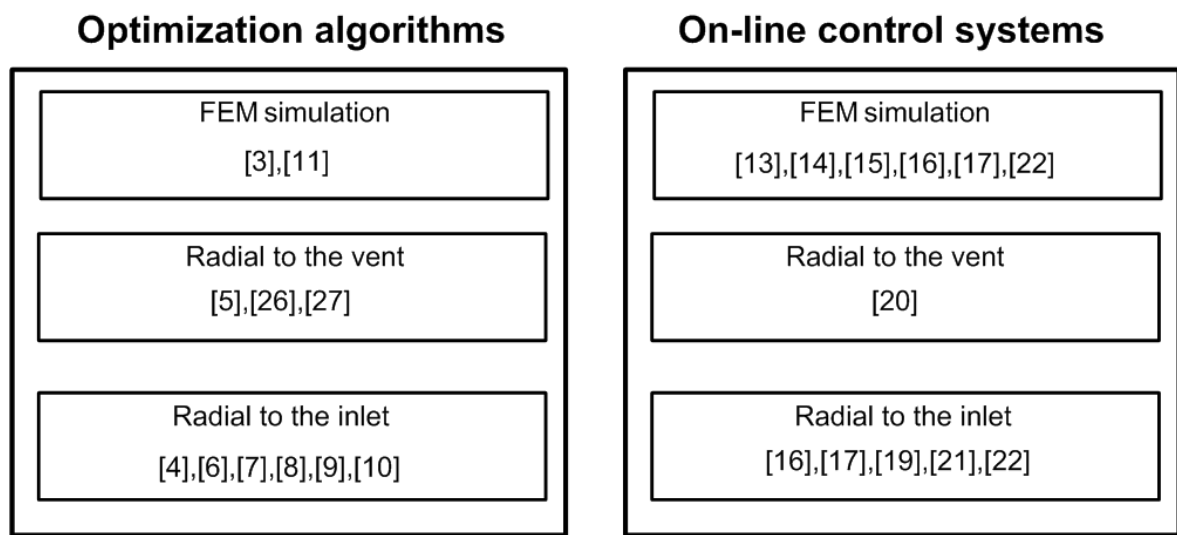


Fig. 3 Diagram summary of the criteria for optimum flow front used in other studies.

## 2 Objective and Outline

The main aim of this paper is to define what the optimum advance front shapes are for use in optimization algorithms, control algorithms or PPI's. In this sense, other studies have used three criteria of optimum advance front that can best be summed up in two. On the one hand, there is the radial nature of the advance front compared to the injector, this being ideal for a simulation in isotropic models, and on the other hand, the radial nature with respect to the vent. Both criteria are valid because the first loosely models the behavior of the flow while the second minimizes the likelihood of occurrence of dry areas during filling. However, both criteria cannot coexist because they are opposites (see Fig. 2), although both are certain and useful, as demonstrated in studies. This implies that it is necessary to have a new definition of what the optimum advance front shapes are. In this sense, the optimum advance front shape is neither radial from the injector nor radial from the vent, but a continuous deformation of one

1 over the other, i.e. when the flow is near the injector, the latter should be radial to it, but when  
2 the flow is near the outlet this flow must be radial, but to the outlet. This continual  
3 deformation is known mathematically as *homotopy*. So, in the first part of this paper,  
4 homotopy is mathematically defined in order to define optimum filling in LCM processes.  
5 This definition is based on the continuous deformation of curves. As a result, one gets what  
6 has come to be called a homotopy map, which defines what the optimum filling phase should  
7 be like.  
8

9 The second part of this article describes how to construct an ideal configuration space to be  
10 used as a computational context for optimization algorithms, on-line control of a process or  
11 PPI indices. This is constructed in the same way that a FPTS is constructed (see [24]), i.e.,  
12 considering the normalized time in which the flow should reach each node. The result is a  
13 space where, if the advance front shape is optimum, it will appear as a straight line in this  
14 space, whatever its shape in the Cartesian space. This enables us to obtain a comparison with  
15 the benchmark in the most efficient way possible. For example, the homotopy concept, along  
16 with its computational context, is used to modify the numerical indices proposed in [26] and  
17 [27], enabling us to measure the suitability of any of the fillings. This new numerical index is  
18 tested for the optimum distribution channels presented in [24],[25]. As a second example of  
19 application, it is proposed that these spaces be used for real time control systems. As this  
20 article shows, the decision-making is done almost intuitively by the controller. At the end of  
21 the article, the conclusions and future work are presented.  
22  
23

### 24 **3 Reference definition based on Homotopy.**

#### 25 **3.1 Previous Assumptions**

26 Flow behavior when injected through a discrete point in isotropic models can be idealized as if  
27 it were a radial filling, whose center is located precisely in the injection nozzle. This model has  
28 been used extensively in other studies (see [4], [6], [7], [8], [9], [16], [17], [19], [21] and [22]).  
29 In these studies, one can define what the filling is like as seen from the injector.  
30  
31

32 Assumption 1: "*Filling as seen from the injector*"  
33

34 "The filling of a mold, as seen from the injector, behaves radially to the latter."  
35

36 As opposed to this concept, the optimum filling criterion that determines the shape of the  
37 advance front is based on the opposite effect, that is to say the shape of flow front should be  
38 radial, but seen from the vent. This is the criterion used in control algorithms and numerical  
39 indices (see [5], [20], [26] and [27]). In these works, one can define what the filling should be  
40 like as seen from the vent.  
41  
42

43 Assumption 2: "*Filling as seen from the vent*"  
44

45 "The filling of a mold, as seen from the vent, must always be radial to the latter."  
46

47 As we can see through these assumptions, the two are opposite, yet both are true or at least we  
48 should like them to be. This implies that it is not possible to obtain a real filling based solely  
49  
50  
51  
52  
53  
54  
55  
56  
57  
58  
59  
60  
61  
62  
63  
64  
65

on one of the two criteria: it should be a combination of both. In other words, the flow front should be radial to the injector when it is near to it, but radial to the vent when the flow front is near it. Thus, a proper definition of an optimum flow front shapes could be:

Assumption 3: "***Proper flow front shapes during filling***"

"An adequate filling is one whose flow front shapes are a continuous deformation of the filling as seen from the injector towards the filling as seen from the vent whose radial nature depends on the proximity of the flow front to each one of them."

Thus, the ideal behavior is neither seen from the injector, nor seen from the vent, but is a continuous deformation of one over the other. When the flow front is near the injector, its shape should be nearly radial to it, but when we are near the vent, the flow front should be almost radial to the vent. This concept of continuous deformation is known mathematically as *homotopy*, that is to say, given two continuous mappings, it is said that they are homotopic (from the Greek *homos* = same and *topos* = place) if one can be "continuously deformed" into the other. This ideal flow behavior based on homotopy has been called "*homotopy map*", where all flow front shapes are contained. Prior to the definition of how to compute a homotopy map, we shall make a topological definition of LCM processes.

### 3.2 Topological definition of LCM processes

All molds used in LCM processes are limited by the contour of the mold. Thus, the mold can be defined as an enclosed and connected region  $\Omega \subset \Re^3$ . Assuming that the outer perimeter of the mold ( $\partial\Omega$ ) can be parameterized by means of a closed curve where  $\gamma^*(u) = (x(u), y(u), z(u))$  for  $u \in [0,1]$  where  $\gamma^*(0) = \gamma^*(1)$ , while for any  $u, v \in (0,1)$  if  $\gamma^*(u) = \gamma^*(v)$  then  $u = v$ . The mold filling can be defined as a curve  $\gamma: (0, T] \rightarrow C_{0,1}([0,1], \Omega)$  where the space  $C_{0,1}([0,1], \Omega)$  consists of injection applications for the interval  $[0,1]$  in mold  $\Omega$ , i.e.  $\gamma_t(0) = \gamma_t(1)$ , interpreting that for  $\gamma(t) = \gamma_t: [0,1] \rightarrow \Omega$ .

At each instant in time,  $t \in [0, T]$ , the curve  $\gamma_t$  represents the advancing front where  $\gamma_t = \gamma^*$  meaning that for  $t = T$  the mold  $\Omega$  is completely filled and,

$$\lim_{t \rightarrow 0} \gamma_t = \gamma_0, \quad \lim_{t \rightarrow T} \gamma_t = \partial\Omega$$

where  $\gamma_0(u) = (x^*, y^*, z^*)$  is a curve that has a constant value, called the point of interest (see Fig. 4).

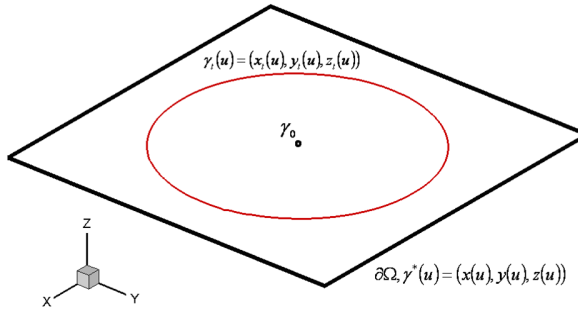


Fig. 4 Mathematical definition of LCM processes. Point of interest is a point.

In LCM processes where the injector and/or vent is a point, as is the case of rigid countermold processes, RTM, the curve  $\gamma_0(u) = (x^*, y^*, z^*) \forall u \in [0,1]$ , but in processes where the injector/vent may not be a point, as is the case in semi-rigid countermolds, VARTM, RTM-Light and VI,  $\gamma_0(u) = (x^*(u), y^*(u), z^*(u)) \forall u \in [0,1]$ , which means it is not a simple curve  $\gamma_0(u) = \gamma_0(v)$  for  $u \neq v$  but a closed curve  $\gamma_0(0) = \gamma_0(1)$  (see Fig. 5).

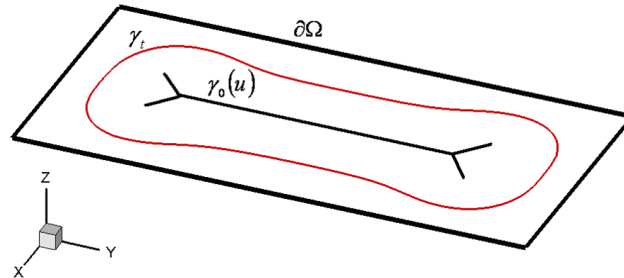


Fig. 5 Mathematical definition of LCM processes. Point of interest is a curve..

### 3.3 Defining a homotopic map for flexible countermold processes.

Focusing on the problem in flexible countermold processes, the advancing front shapes that define the optimum flow behavior between the contour of the mold,  $\gamma^*(u)$ , and the point or curve of interest,  $\gamma_0(u)$ , which are defined in  $\mathbb{R}^3$  as  $\gamma^*(u) = (x^*(u), y^*(u), z^*(u))$  and  $\gamma_0(u) = (x_0(u), y_0(u), z_0(u))$  respectively, are defined as a continuous deformation between the two curves, i.e.:

$$H(\gamma^*, \gamma_0) = \gamma^* t_H + \gamma_0(1 - t_H)$$

where  $t_H \in [0,1]$  is the intrinsic parameter that controls the deformation, with normalized filling time. The evolution of this intrinsic parameter is linear because must be dependent to their relative position with respect to the origin and destination. This parameter can be defined according to the process to which it is applied. For processes such as VI,  $t_H = [0...1]$ , since the vent is the perimeter of the mold. However, for processes such as VARTM,  $t_H = [1...0]$ , since the perimeter of the mold is the injector.

1  
2  
3  
4 **4 Computational framework based on Homotopy maps**  
5  
6  
7  
8  
9  
10  
11  
12  
13 **and Flow pattern configuration spaces.**

14  
15  
16  
17 **4.1 Flow Pattern Configuration Spaces and their use in calculating the**  
18 **optimum location for the injection nozzles.**

19  
20  
21  
22  
23 One of the most important reflections that can be gleaned from the shortcomings of the  
24 algorithms used in LCM processes, for both on-line control systems and optimization  
25 algorithms, is the need to define tools that are as simple and computationally efficient as  
26 possible. The proper treatment of information may allow better understanding of the process  
27 and in turn reduce the computation time and facilitate the development of the necessary  
28 algorithms.

29  
30  
31  
32  
33 In other fields such as mobile robotics, similar problems are solved using the concept of  
34 configuration space ([23]). This concept seeks to represent the space where algorithms are  
35 calculated, the Cartesian space, an alternative space developed by the parameters to be  
36 optimized or controlled. This concept was first introduced into LCM processes in our previous  
37 work ([24]), its properties and benefits being previously unknown. Application of the concept  
38 of configuration spaces in LCM processes has come to be called "*Flow Pattern Configuration*  
39 *Spaces (FPCS)*". In this paper several variants of these spaces are proposed, based on a fixed  
40 variable  $\theta$  and another free one  $\psi$ . The fixed variable  $\theta$  is based on the radial nature of the  
41 advance fronts, an angle from a point of interest to points defined in the mesh. The first option  
42 analyzed for the free variable  $\psi$  is to consider it as the distance from the point of interest to  
43 the mesh nodes as a rough measure of the time. These spaces are called "Flow Pattern Distance  
44 Spaces (FPDS)." In Fig. 6 there is an example of the result superimposed on the result of the  
45 simulation in the Cartesian space. In this example, the point of interest is the injector. The  
46 second option analyzed as a free variable is the normalized filling time obtained using a Finite  
47 Element simulation. These spaces are called Flow Pattern Time Spaces (FPTS). In Fig. 7 there  
48 is an example of the resulting space where the point of interest is also the injector. Using these  
49 variables it is proposed that two new spaces be built. One is based on reconstruction of the  
50 coordinates on a 2D space, called 2D-FPDS, 2D-FPTS; another one is based on the polar  
51 representation of the variables, called 1D-FPDS, 1D-FPTS. Fig. 8 shows the construction  
52 diagrams for these spaces.

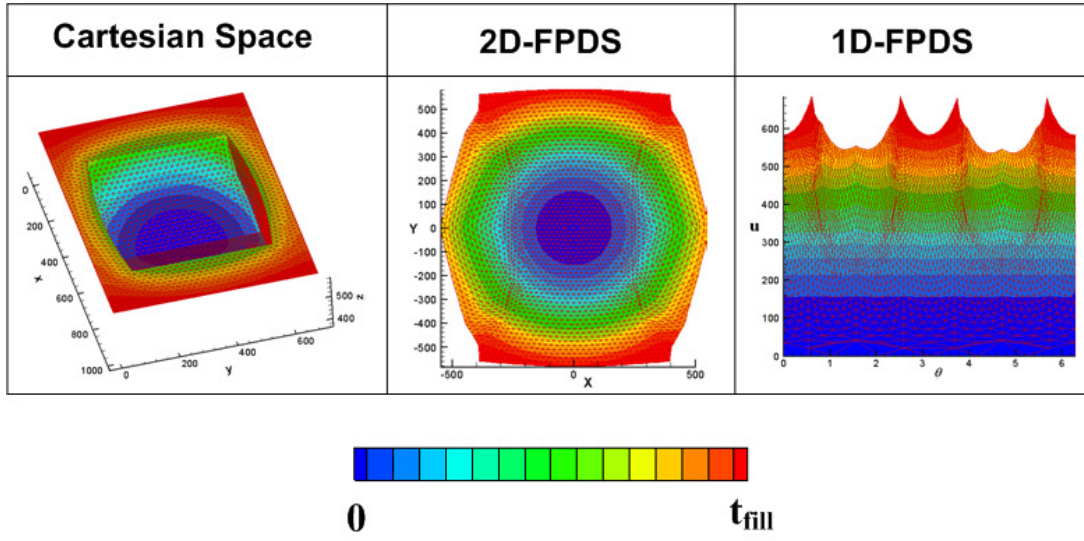


Fig. 6 Example of Flow Pattern Distance Space.

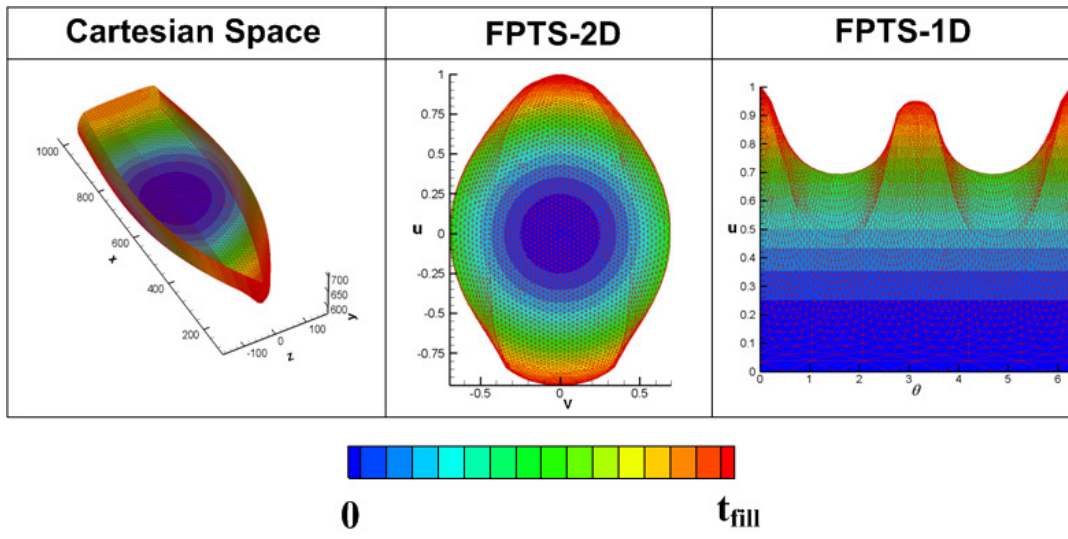


Fig. 7 Example of Flow Pattern Time Space.

### Flow Pattern Distance Space (FPDS)

### Flow Pattern Time Space (FPTS)

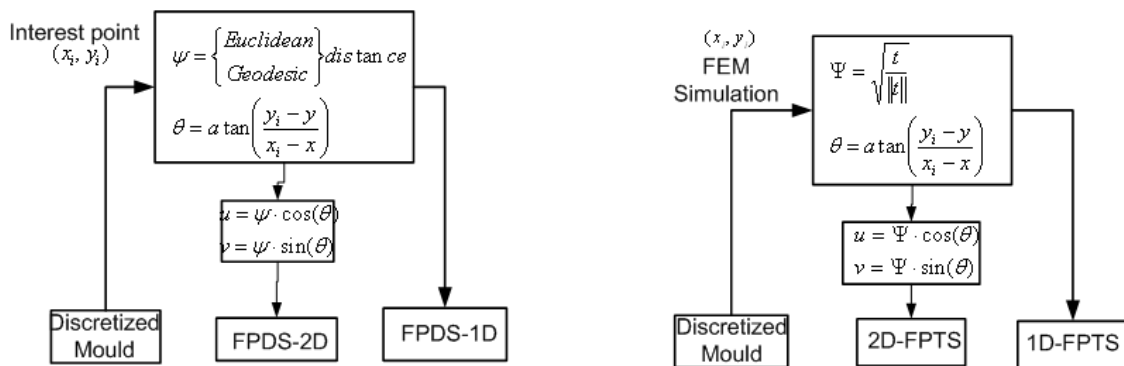


Fig. 8 Construction diagrams.

In both cases, it is possible to reduce the complexity of the area to be dealt with, both in optimization and control algorithms, inherently achieving a reduction in computation time for

the proposed algorithms. This complexity is reduced not only by reducing the dimension of the space, but also the coordinates of these spaces are the variables to be optimized or controlled. [25] focuses on the use of these spaces in optimization algorithms to calculate the distribution channels for VI processes. In these processes, as in all LCM processes, one of the priority objectives of the filling phase is for the flow to reach the vent at the same instant in time, thus ensuring complete impregnation of the preform. In this process, the optimization problem is considerably more complex than the processes commonly discussed in other works, RTMs, due to the characteristics of the injector. The vent must be placed around the perimeter of the mold to be infused, in order to achieve the best distribution of the pressure gradient and thereby minimize the areas of different permeability caused by the flexible countermold, which is a plastic bag. So the first premise proposed in [25] is that the vent should be positioned in the contour of the mold. The second premise can be obtained from the definition given in [26] and [27]. In these works, the ideal advance front must be equally distant from the vent (contour) at every instant of time in order to be considered optimum. This enables us to consider the curve that is going to define the optimum distribution channel to be equally distant, because the optimum distribution channel can be considered to be the advance front itself at the initial time of filling. Thus, to determine what the optimum shape and location of the distribution channel is, we only have to apply the Delaunay triangulation of a Euclidean space, in this case the 2D-FPDS one. Since in this space the coordinates are distances, the optimum solution is obtained without any kind of iteration, obtaining the result in a few seconds. As you can see from the example in Fig. 9, the algorithm gives a degree of freedom and the resolution of the distribution channel can be chosen. As shown in [25], the higher the resolution, the lower the filling time; in addition the flow reaches the vent in a more uniform way. However, the waste of resin trapped in distribution channels is greater and so is the complexity of the channel to be set up.

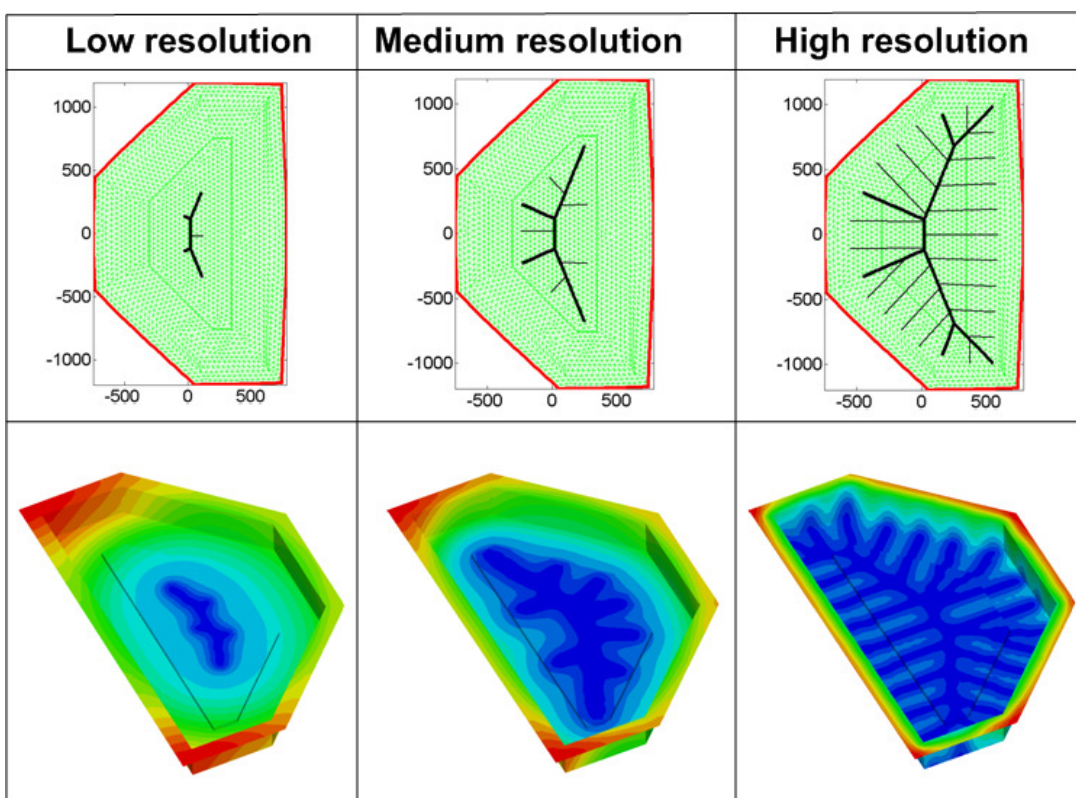


Fig. 9 Example of optimum distribution channel for a geometry of 2.5D.

## 4.2 Techniques for calculating a homotopy map in a Flow Pattern Configuration Space.

Applying the homotopy concept of 2.5D geometries is complicated, and we should indicate which paths the deformation must follow. However, it is simple if we apply it in the 1D configuration spaces proposed in [24], as this reduces the number of dimensions used in the definition of the curves  $\gamma^*(u)$  and  $\gamma_0(u)$ , whatever the geometry of the mold. In addition,  $\gamma_0(u)$  is always represented in these kinds of spaces as a straight line placed at the origin with coordinates at zero,  $\gamma_0(\psi, \theta) = 0 \forall \theta \in [0 \dots 2\pi]$ ,  $\psi$  being the free parameter, with normalized time for the 1D-FPTS and distance for the 1D-FPDS (see [24]). Thus the homotopy deformation defined in the 1D-FPCS looks like:

$$H(\gamma^*, \gamma_0) = \gamma^* t_H \text{ where } \gamma_t = f(t_H, \theta).$$

In Fig. 10 there is an example for a boat using the FPDS. The method to be followed is as follows. Given a mold in the Cartesian space, the transformation is performed to 1D-FPDS. In this space the contour continuously deforms with respect to the origin, which would be vents or injectors depending on the process. Once done, if we represent these shapes again in the Cartesian space we will get what is to be called a *homotopy map*, i.e., the optimum advance front shapes for the filling of the mold.

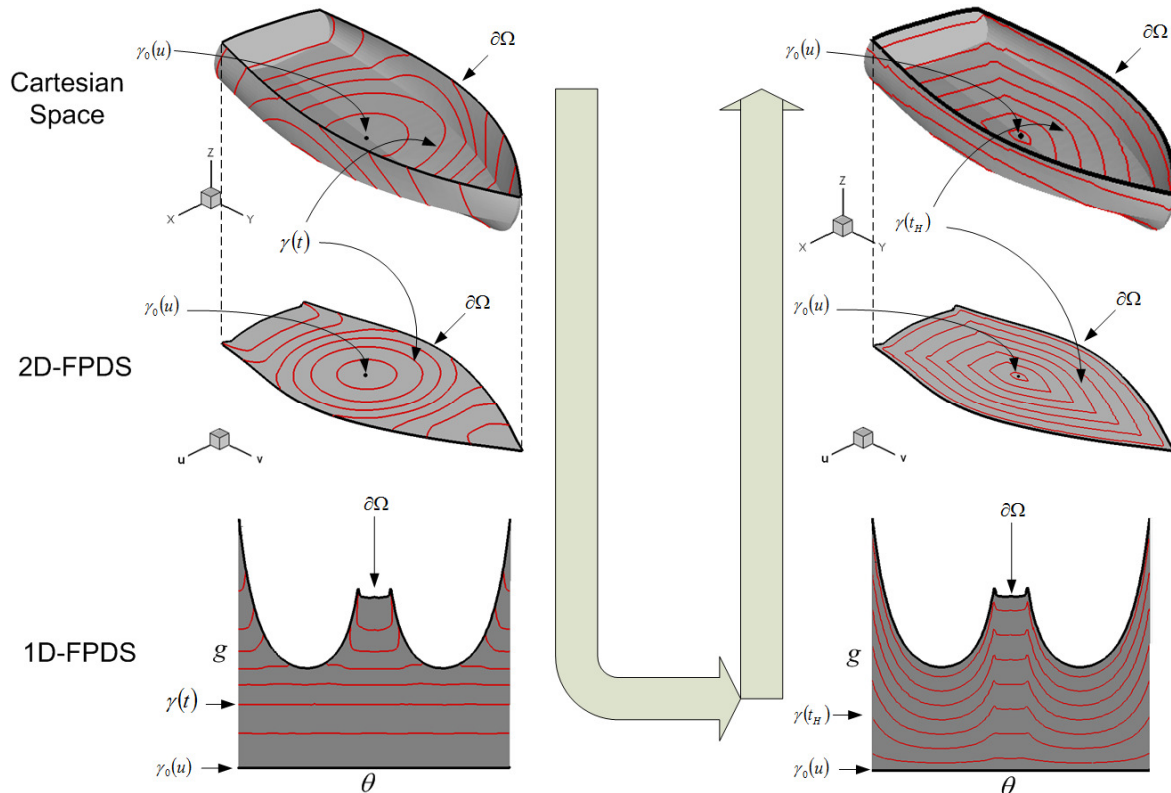


Fig. 10 Method for calculating a homotopy map.

Treatment of the functions  $\gamma^*(u)$  and  $\gamma_0(u)$  is also known as *morphology*, since what is being carried out is the continuous transformation of one function into another. This concept is widely used in fields such as 3D animation for *morphing*. In these cases, continuous functions are usually curves or parametric surfaces defined by means of Beziers, B-Splines or NURBS (see for example [31]). Also, *morphology* is usually applied to meshed objects as in [32]. In these cases it is necessary to define what path is to be followed for each node in the mesh, from the initial position to the final position. These paths are called *isolines*. In the case of using FPCS, the isolines are straight lines that come together for each angle  $\gamma^*(u)$  and  $\gamma_0(u)$ . In the case of using FPDS, they are Euclidean or geodesic lines. When using FPTS's, the lines generated are also geodesic but considering the flow behavior. In the two cases, each line defines the ideal path that each point of the advance front should follow (see Fig. 11).

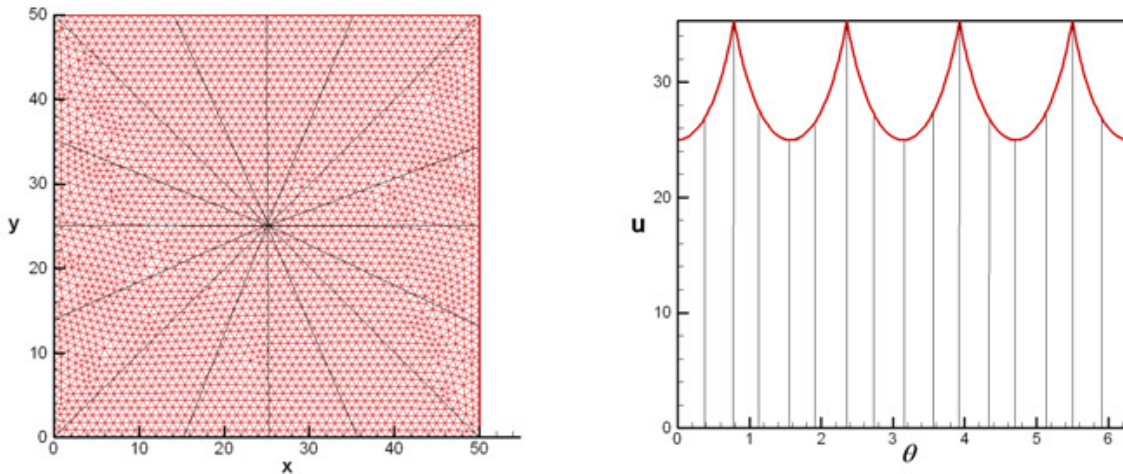


Fig. 11 The Euclidean/geodesic distances calculated from the FPDSs are the isolines that define a homotopy map

The calculation of the homotopy map via the mesh can be also obtained simply irrespective of whether we use the 1D-FPTS or FPDS. To do so we have to calculate the parameter  $t_H$  for each node, i.e. the normalized time in which the flow should arrive at it. Given a node  $n$ , the normalized time is the relationship between the distance from the node to the origin,  $d_n$ , with the isoline to the contour passing through this node,  $d_{iso}$  (see Fig. 12), i.e.:

$$t_H = d_n / d_{iso} \text{ where } t_H \in [0,1].$$

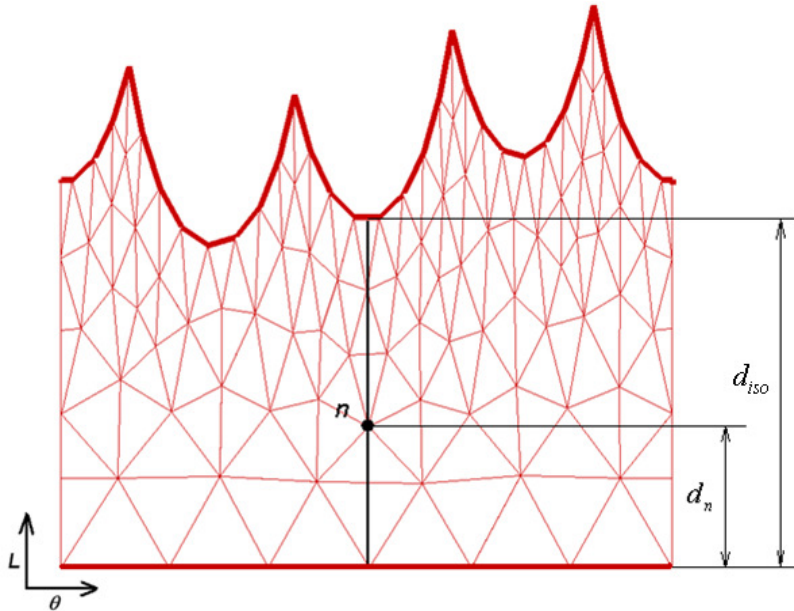


Fig. 12 Calculation of normalized time in which the advance front should reach each node

The result is a filling with normalized time where the advancing front shapes are a continuous homotopic deformation. Fig. 13 shows several examples of optimum flow shapes made using the 1D-FPDS. As shown in the advancing front shapes obtained in the examples of rows 1,2 and 4, the advancing front shapes are very different from what a real filling would be, whereas in the case of row 3, a square with the main optimum branch obtained in [25], the advance front shapes are closer to what a real filling might be. This is because the optimization method proposed in [25] seeks to obtain equal distances, and this implies that in the ideal case, a  $\Delta t_H$  causes a proportional increase in the position of the advancing front in all directions. Fig. 14 shows examples of optimum flow shapes from injectors with the shapes obtained by the method proposed in [25]. As one can see in these examples, as the injector's resolution increases, the simulated advance flow front shapes become more similar to the ideal homotopic filling than those obtained by means of the homotopic map.

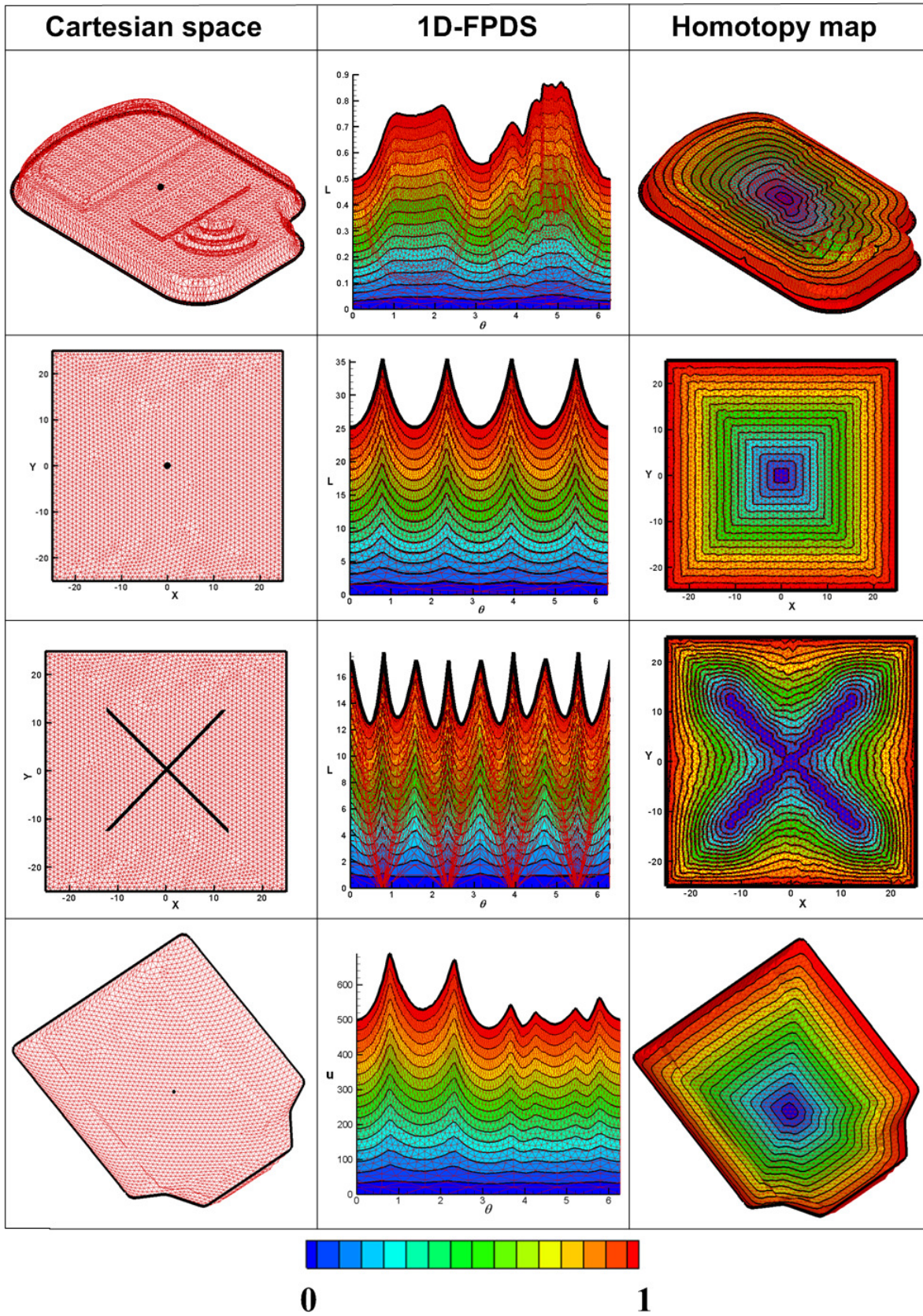


Fig. 13 Examples of homotopic maps for flexible counter-mold processes with the FPDS.

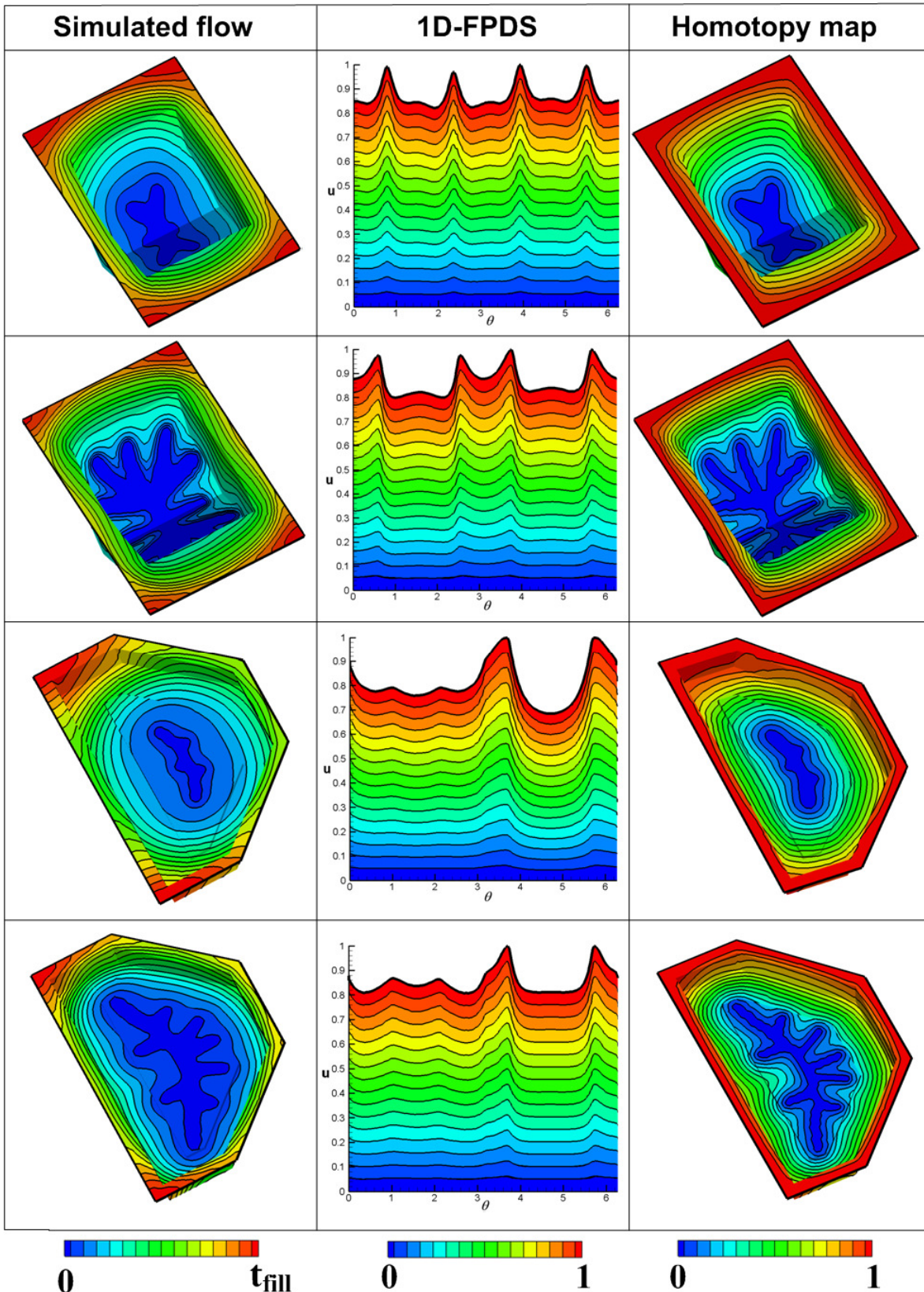


Fig. 14 Examples of homotopic maps for flexible countermold processes.

### 4.3 Construction of configuration spaces based on homotopic flow behavior. Flow pattern Homotopy Space (FPHS).

As explained in the introduction, the computation time in both the optimization algorithms and on-line control is a concept to be reduced. To efficiently measure how much the ideal advancing front shape changes with respect to the real one, we can use the concept of configuration space applied to this case. Thus, using a homotopic map where  $\gamma_t = f(t_H, \theta)$  and  $t_H \in [0,1]$ , the normalized time in which the flow should reach each node can be selected, as in the FPTS, as the free parameter for the construction of the configuration space:

$$\Psi(u) = f(t_H / \|t_H\|)$$

where  $\|t_H\|$  is the infinite standard or the maximum standard as in:

$$\|t_H\|_\infty := \max(t_H) \text{ where } t_H \geq 0.$$

and for spaces based on homotopic maps this will always be equal to one. At each instant of time,  $t_H \in [0,1] \rightarrow \Psi(u) \in [0,1]$ . In this sense, the resulting space complies with:

$$\lim_{t \rightarrow 0} \Psi(u) = 0 = \gamma_0, \quad \lim_{t \rightarrow T} \Psi(u) = 1 = \gamma^*$$

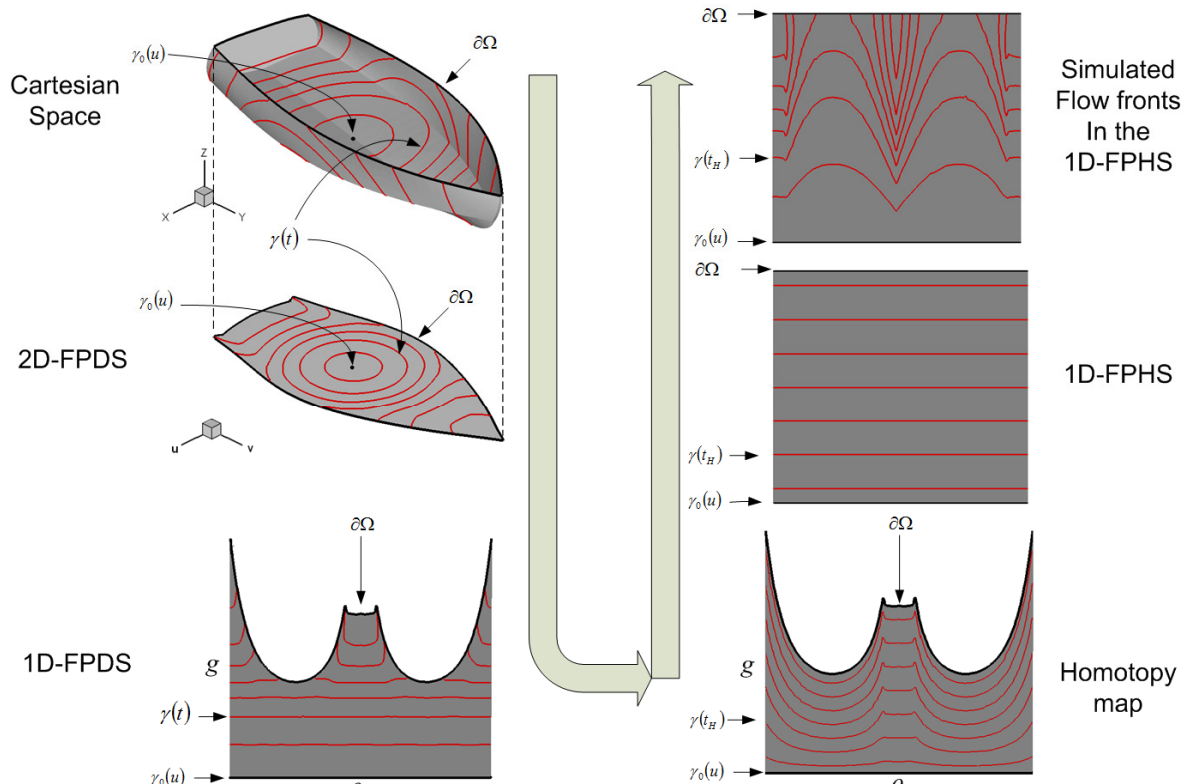


Fig. 15 Flow Pattern Homotopy Space (FPHS).

The resulting configuration space is called *Flow Pattern Homotopy Space (FPHS)*, and both 2D and 1D versions can be constructed. In this space, the representation of the real advance front  $\gamma_t(u) \rightarrow \gamma_t(\Psi(u), \theta(u))$  will be a circle or a straight line if the advancing front shape corresponds to the one predefined in the homotopic map. Fig. 15 shows how to construct a FPHS using the FPDS obtained for the boat from a point placed in the center of masses. Thus, using the 1D-FPDS, the homotopic map is generated, and from the standard times  $t_H \in [0,1]$ . If we show the simulation of the boat developed in the Cartesian space in the 1D-FPHS it is easy to determine how it differs from the ideal one. Fig. 16 shows a summary diagram of how to construct the FPHS's.

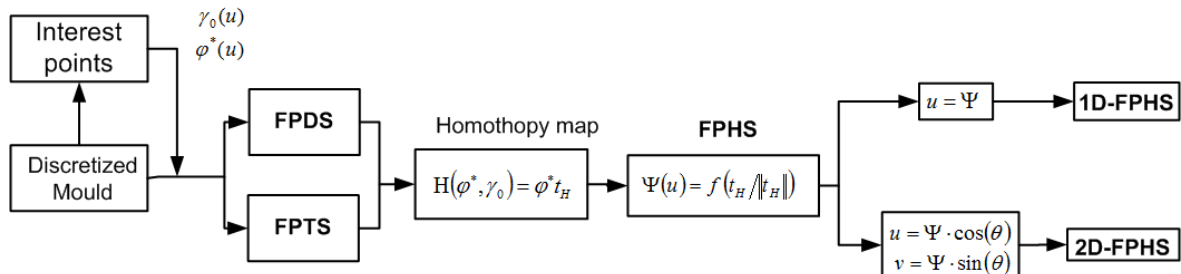


Fig. 16 Construction of flow pattern spaces based on homotopic maps (FPHS).

Fig. 17 shows examples of these types of spaces calculated on the discrete mesh. In particular, in rows 1 and 2 one can see a square mold filled from a point located at the centroid and from the optimum main branch obtained in [25]. As we can observe, the advance fronts have shapes closer to being a straight line in the 1D-FPHS and closer to a circle in the 2D-FPHS, when the injector is cross-shaped and produces better equidistance with the contour. The same applies to the example of Fig. 17, row 3 and 4, where in this case the example is a 2.5D mold.

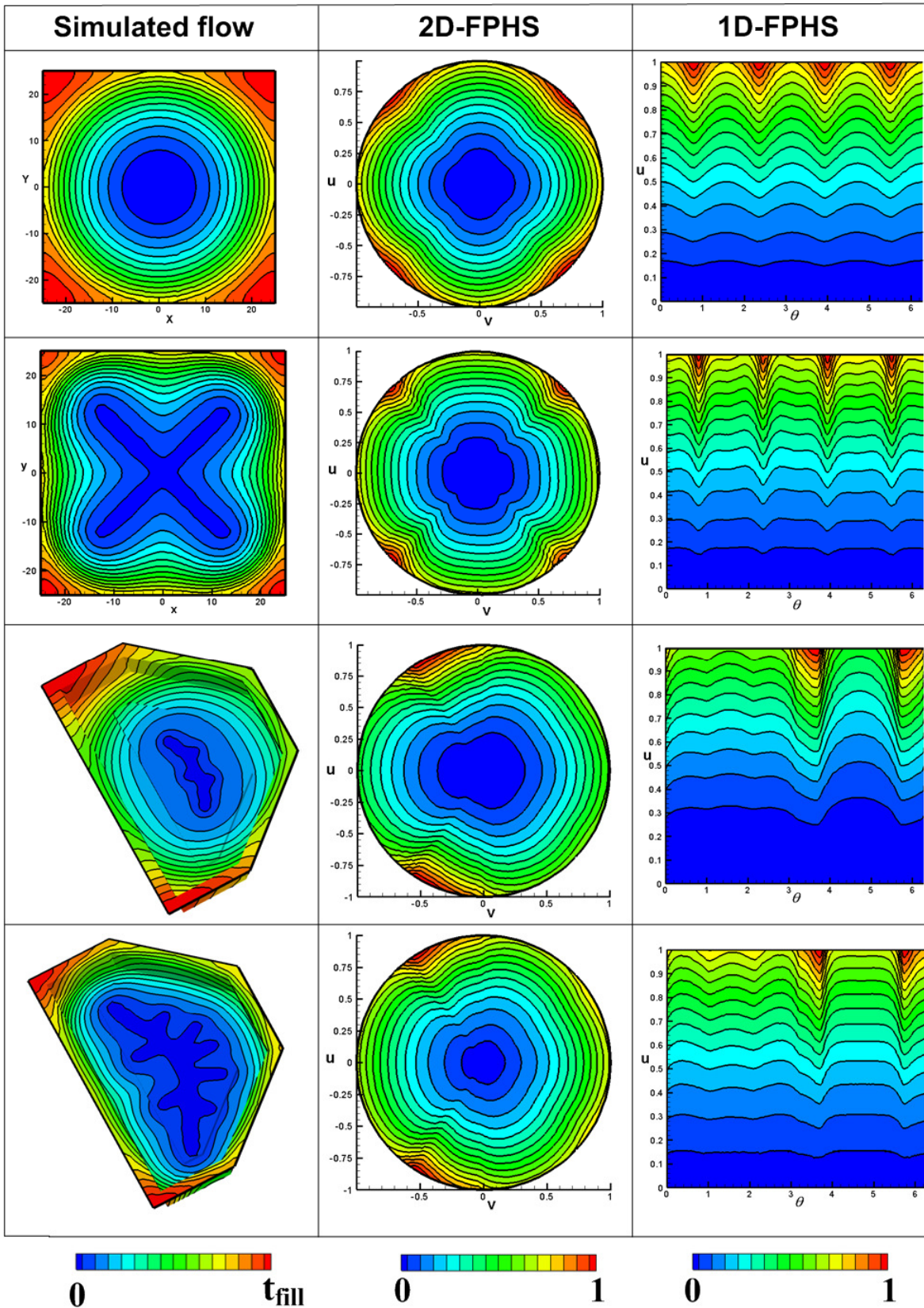


Fig. 17 Construction of flow pattern spaces based on homotopic maps for isotropic models.

## 5 Examples of application

This section aims to show, by way of example, some possible applications that both homotopic maps and Flow Pattern Homotopic Spaces can have. The first one involves modifying the indices proposed in [26] and [27] to measure how suitable the advance front shapes are for flexible counter-mold processes.

### 5.1 Process Performance Index (PPI) based on homotopic flow behavior

By using the 1D-FPHS's, we can compare the representation of the advance front with a straight line, whatever the size and shape of nozzles, thus reducing the computation time. Thus, modifying the indices proposed in [26] and [27], in the part where the idealness of the shape of the advance front shape is calculated, equidistant to the vent, we can obtain a PPI based on these advance front shapes. Thus, the index that enables us to measure how good the filling is for semirigid counter-mold processes, considering the homotopy as a criterion for optimal front shape, would be:

$$Q_H = \frac{\sum_{k=1}^m \sqrt{\frac{\sum_{i_k=1}^{n_k} (\gamma_{ik} - \bar{\gamma}_k)^2}{n-1}}}{m} = \frac{\sum_{k=1}^m h_k}{m} = \frac{H}{m}$$

where:

$Q_H$  is the total filling index.

$h_k$  is the intermediate index for each advance front.

$m$  is the number of advance fronts considered.

$n_k$  is the number of nodes that define the advance front  $k$ .

$\gamma_{ik}$  is the normalized time of node  $i$  in the 1D-FPHS located on the advance front  $k$ .

$\bar{\gamma}_k$  is the average of the advance front times represented in the 1D-FPHS.

$H$  is the index of dispersion for the advance front in the 1D-FPHS.

This index can be completed introducing the filling time as in [26] and the incubation time as in [27].

By using this PPI in the FPHS, it can be applied in the same way and with the same computational costs if the mould is 2D or 2.5D or if the mold is RTM, discrete inlets/outlets, or is an VI, distribution channels. The PPI proposed in [26] and [27] only is valid for 2D RTM moulds because use the Euclidean distance, see [24].

Fig. 18 shows several simulated examples of how the index evolves when the resolution of the injector as defined in [25] increases. As we can see, the examples of the column 1 and 2, the higher the resolution of the injector, the lower the  $H$  index, which measures the idealness of the advance front. Not only does this indicator of the  $Q_H$  index decrease as we introduce more complexity, but also the maximum filling time falls (see [25]).

It is also interesting to note the dependence of the result obtained on the geometry used. Looking at the example of the pool of the column 3, the homotopy index of the pool is smaller compared with the indices obtained in the examples in column 1 and 2, even if simply the optimum main branch from [25] has been used. This is because although the pool model may seem more complex, in truth getting the advance front shapes to be homotopic is simpler because their shape in the 2D-FPDS is smoother and simpler to obtain to achieve an inlet/outlet equidistance.

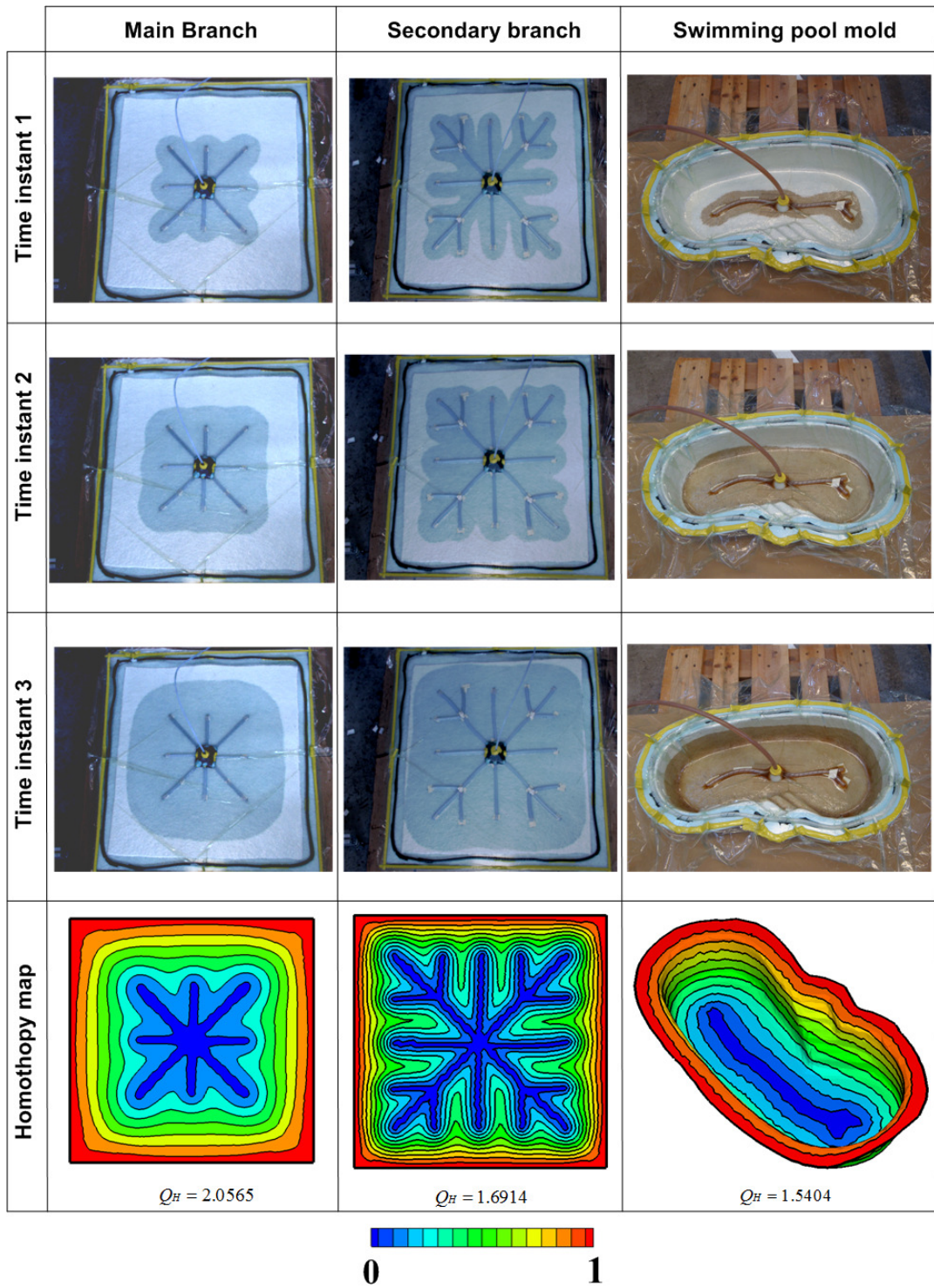


Fig. 18 Evolution of the index of suitability for the flow front shape in different filling strategies.

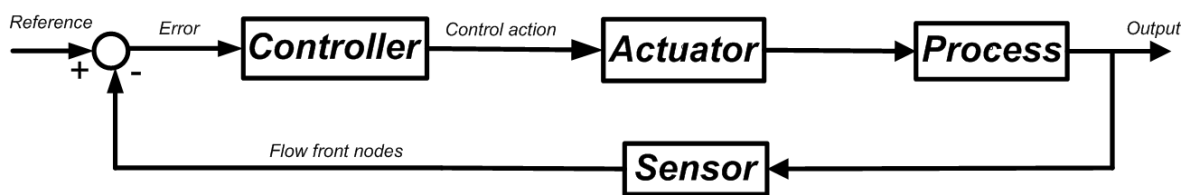
1  
2  
3  
4  
5  
6  
7  
8  
9

## 5.2 Application of the FPHS in the on-line control of sensorized flexible counter-mold processes by means of artificial viewing techniques.

10 Artificial viewing, and in particular cameras, are devices that show the amount of light there is  
 11 on a scene. These devices are widely used in industry for inspecting quality, and in many  
 12 applications such as surveillance cameras, webcams, robotics, etc. ([34]). The cameras contain  
 13 a chip composed of an array of light sensors. Depending on the technology used to make them,  
 14 these can be divided into two groups: CMOS's (Complementary Metal Oxide Semiconductors)  
 15 and CCD's (Charge Coupled Devices). These sensors consist of a standardized number of  
 16 pixels: 640x480, 1400x1000, etc.  
 17

18 Using the camera parameters, we can discover the true dimensions of 2D scenes. By placing  
 19 the camera parallel to the scene, all one needs to do is to calculate the scale factor. If the  
 20 camera is required to sample 3D scenes, it is necessary to use additional devices that enable us  
 21 to calibrate the true position of the pixels on the scene. There are numerous techniques for this  
 22 purpose: structured light, using a laser, or using known templates placed in the scene ([34]).  
 23

24 In our previous work, [24], [33], the idea was proposed of considering the camera sensor to be  
 25 an array of nodes, and relate them to one another in the same way that the nodes of the mesh  
 26 used in finite element simulation (FEM) are related. Through the relationship between pixels,  
 27 it would be possible to define any type of finite element geometry, triangle, square, hexagon,  
 28 etc. Usually, triangular finite elements are used in simulation. By doing so, one manages to  
 29 sensitize the mold with a 2D or 3D mesh, which can be used and work done with it. In our  
 30 previous works, [35], Camera vision was firstly proposed as a sensor in a classical control  
 31 loop, see Fig. 19, for VI processes. In this case, camera and artificial vision techniques  
 32 determines the flow front nodes in each time instant. This nodes must be compared in real time  
 33 with the reference for this time instant. The resulting error is used by the controller to compute  
 34 the required action. In this control loop, the comparision of the flow front nodes in each time  
 35 instant gives an excessive time, reducing the properties of the control. To solve this problem,  
 36 in [35] was used CAD techniques to reduce the number of flow front nodes.  
 37



54 In order to reduce the computational costs without loose precision in the flow front, in [24]  
 55 was proposed of simulating the camera mesh and using the results of the simulation to  
 56 construct a FPTS. As the nodes and the pixels are interconnected, the true filling monitored by  
 57 the camera is displayed in this space instantly. Since this space is configured so that the  
 58 advance front is represented with a straight line if it corresponds to the simulation, decisions  
 59 can be made by the controller in real time.  
 60

In the same way that a FPTS is constructed for use in real-time control systems, an FPHS can be constructed where the control benchmark is provided by the homotopy map. Since the operation of constructing this space is done off-line, the comparison of the real advance front with the homotopic one is immediate because the ideal front shape shall be represented as a straight line over this space, see Fig. 20.

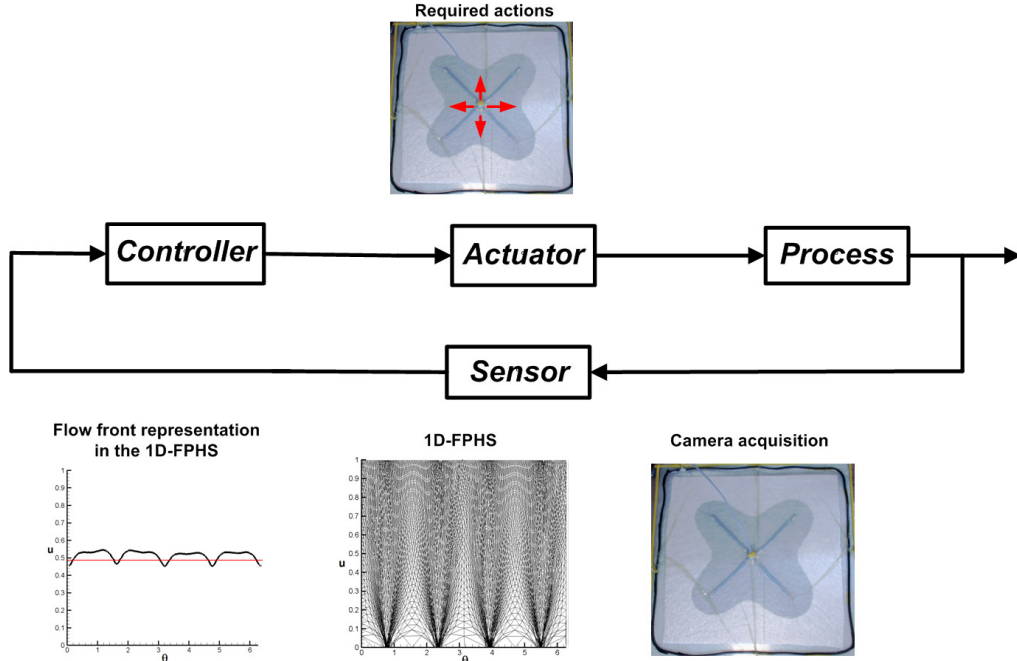


Fig. 20 Loop diagram of control by means of FPHS and homotopy map.

If we compare both control loops, a classical control loop depicted in Fig. 19, and the proposed in Fig. 20, we can see that the reference disappears because is intrinsically allocated in the 1D-FPHS, avoiding the comparison and with the consequent computational costs reduction.

## 6 Conclusions and future studies

This article has presented how to mathematically model the behavior of optimal flow for LCM processes, specifically for flexible countermold processes. This behavior is defined as the homotopy between natural filling seen from the injector until the desired filling seen from the vent. This definition is justified since in previous studies ([26] and [27]) the optimum front shape is established as one which is equally distant from the vent at all instants of time during filling. In fact, this desired behavior is the opposite of the natural behavior of the flow, i.e., radial but from the injector. While the first criterion is used to measure how good the filling is ([26] and [27]), the radial flow behavior as seen from the injector is used to find the optimum location of the vent in RTM processes ([6]), placing this at the point furthest away. In fact, as demonstrated in this study, the optimal behavior of the flow is neither radial to the vent nor radial to the injector, but a continuous deformation behavior of one over the other. This continual deformation is defined mathematically as *homotopy*. So, given an injector and a vent in flexible countermold processes, homotopy is defined as a continuous deformation between

1  
2  
3  
4  
5  
the injector and vent. The resulting advance fronts generate what in this study has been called a  
homotopy map, defining the shapes of the advance front not according to time, but according  
to their relative position with respect to the origin and destination.

6  
7  
8  
9  
10  
11  
12  
13  
14  
15  
16  
17  
18  
19  
20  
13  
21  
22  
23  
24  
25  
26  
27  
28  
The correspondence between the flow front shape's homotopic behavior and the real advance  
front shape depends on how optimal the positions of the injector and the vent are, enabling us  
to use this criterion in optimization algorithms. In this article we used the optimal shape and  
position of the injector for VI processes, calculated in [24], [25], where the criterion was to  
make the injector equally distant from the contour. If we get it to be equally distant, as in the  
simple case of trying to fill a circular mold by placing the injector in the center, this would  
imply that the homotopic behavior would be the real one. This is why the more we increase the  
resolution of the injector; the closer the real flow front shapes resemble the homotopy map.  
This shows the suitability of the homotopy criterion as an optimum measurement of the flow  
front shapes. As an example of application, it is proposed that the indices proposed in [26] and  
[27] be modified so that the advance front shapes are the homotopic ones. In order to  
efficiently carry out the calculation and thereby extend its application to on-line control  
algorithms, it is proposed that a new configuration space be developed, called *Flow Pattern*  
*Homotopy Space (FPHS)*. This space is obtained in the same way as the FPTS's proposed in  
[25], but in this case, instead of using a simulation, the homotopy map is used. In this new  
space, if the advance front is the ideal shape, its representation is a straight line, facilitating  
and in turn reducing the computation time for the comparison.

29  
30  
31  
32  
33  
34  
35  
Although the concept of homotopy for defining the optimum advance front is applicable to any  
LCM process, the homotopy map can only be obtained for processes where the injector or the  
vent is a curve and not when both are points. This is because it would be necessary to work  
with curves, thus providing a degree of freedom in the definition. How to make continuous  
open deformation curves is a current discussion in mathematics and it is our future line of  
work.

## 38 39 40 41 References

- 42 [1] Cai Zhong. *Analysis of mold filling in RTM process*. J Compos Mater 1992;26(9):1310-38.  
43 [2] Young WB. *Gate location optimization in liquid composite molding using genetic*  
44 *algorithms*. J. Compos Mater 1994;28 (12):1098-113.  
45 [3] Mathur R, Fink BK, Advani SG. *Use of genetic algorithms to optimize gate and vent*  
46 *locations for the resin transfer molding process*. Polym. Compos 1999;20(2):67-78.  
47 [4] Lin M., Murphy M., Hahn H., *Resin transfer molding process optimization*. Compos. Part  
48 A. 31(4); 361-71. 2000.  
49 [5] Luo J, Liang Z, Zhang C, Wang B. *Optimum tooling design for resin transfer molding*  
50 *with virtual manufacturing and artificial intelligence*. Compos Part A 2001;32:877-88.  
51 [6] Jiang S, Zhang C, Wang B. *Optimum arrangement of gate and vent locations for RTM*  
52 *process design using a mesh distance-based approach*. Compos Part A 2002;33:471-81.  
53 [7] Gokce A, Hsiao K, Advani SG. *Branch and bound search to optimize injection gate*  
54 *locations in liquid composite molding process*. Compos Part A 2002;33:1263-72.

- [8] B.Yoon Kim, G.Joon Nam, J.Wook Lee, *Optimization of filling process in RTM using a genetic algorithm and experimental design method*. Polymer Composites Vol.23, N°1, pp.72-86, 2002.
- [9] R. Mathur; S. G. Advani; and B. K. Fink, *A Real-Coded Hybrid Genetic Algorithm to Determine Optimal Resin Injection Locations in the Resin Transfer Molding Process*, Computer Modeling in Engineering and Sciences, Vol. 4, No. 5, pp. 587-602, 2003.
- [10] Gokce A., Advani S. *Simultaneous gate and Vent location optimization in liquid composite molding processes*. Material manufacturing process 19(3);523-48. 2004.
- [11] Hsiao K-T, Devillard M., Advani S.G. *Simulation based flow distribution network optimization for vacuum assisted resin transfer molding process*. Model Simul. Mater. Sci. Eng. 2004;12:175-90.
- [12] J.F.A.Kessels, A.S.Jonker, R.Akkerman, *Optimising the flow pipe arrangement for resin infusion under flexible tooling*. Compos. Part A 38, 2007, pp. 2076-2085.
- [13] Lee C., Rice B., Buczek M., Mason D., *Resin transfer molding process monitoring and control*. In proc. of international sampe symp. and exhibition. Vol 43(1);pp 231-42. 1998.
- [14] Bickerton S., Stadefld H., Steiner K., Advani S., *Design and application of actively controlled injection schemes for resin-transfer molding*. Compos. sci. tech. 61(11);1625-37;2001.
- [15] Nielsen D., Pitchumani R., *Intelligent model-based control of preform permeation in liquid composite molding process, with on-line optimization*. Compos. Part A. 32(12) 1789-803. 2001.
- [16] Nielsen D., Pitchumani R., *closed-loop flow control in resin transfer molding using real-time numerical process simulations*. Compos. sci. tech. 62(2) 283-98. 2002.
- [17] Nielsen D., Pitchumani R., *Control of flow in resin transfer molding with real-time perform permeability estimation*. Polym. Compos. 23(6);1087-110;2002.
- [18] Lawrence J., Hsiao K., Don R., Simacek P., Estrada G., Sozer M., et al. *an approach to couple mold design and on-line control to manufacture complex composite parts by resin transfer molding*. Compos. part A. 33(7) 981-90. 2002.
- [19] D.Bender, J.Schuster, D.Heider. *Flow rate control during vacuum-assisted resin transfer molding (vartm) processing*. Compos. Sci and tech. pp. 2265-71. 2006.
- [20] Modi D.,Correia N., Johnson M., Long A., Rudd C. and Robitaille F. *Active control of the vacuum infusion process*. Compos. Part A. 38, 1271-1287. 2007.
- [21] R.J.Johnson, R.Pitchumani. *Flow control using localized induction heating in a VARTM process*. Compos. Sci. and tech. Vol 67, Is 3-4, pp 669-684, 2007.
- [22] Nalla A.R., Fuqua M., Glancey J. and Lelievre B., *a multi-segment injection line and real-time adaptative, model-based controller for vacuum assisted resin transfer molding*. Compos. Part A. 38, 1058-1069. 2007.
- [23] J. C. Latombe, *Robot Motion Planning*. Kluwer Academic Publishers, 1991.
- [24] N.Montés, F.Sánchez. *A new computational tool for liquid composite molding process design based on configuration spaces*. Vol. 41, Is 1,pp 58-77. January 2010
- [25] N.Montés, F.Sánchez. *A geometry based simplified approach for the computational formalisation of the resin channel distribution design in resin infusion process*. Polymer composites. Under review.
- [26] Jiang S. Zhang C., Wang B. *A process performance index and its application to optimization of the RTM process*. Polym. Compos 2001;22(5):690-701.
- [27] F. Sánchez, J.A. García, F. Chinesta, Ll. Gascón, C. Zhang, Z. Liang, B. Wang, *A process performance index based on gate-distance and incubation time for the*

- optimization of gate locations in liquid composite molding processes.* Compos Part A, 903-912, Vol.37/6, 2005.

  - [28] Ramis X., Salla JM. *Efect of the inhibitor on the curing of an unsaturated polyester resin.* Polymer 1995;36(18):3511-21.
  - [29] Rouison D, Sain M, Couturier M. *Kinetic study of an unsaturated polyester resin containing an inhibitor.* J. Apply Polym Sci. 2003;89:2553-61.
  - [30] Cardona C., Ziae S, Advani SG. *Spatially homogeneous gelation in liquid composite molding.* Polym. Eng Sci 2002; 42(8):1667-73.
  - [31] T.Ju, R.Goldman. *Morphing Rational B-Spline curves and surfaces using mass distributions.* Eurographics 2003.
  - [32] A.W.F.Lee, D.Dobkin, W.Sweldens, P.Schorödes. *Multiresolution mesh morphing.* Proceedings of SIGGRAPH 99. pp. 343-350, August 1999.
  - [33] N.Montés, F.Sánchez, J.Tornero. *Numerical technique for the space discretization of resin infusion mold sensing with artificial vision.* Int. J. of Material Forming Vol 1, Sup. 1, pp 923-926. 2008.
  - [34] Bernd J., Horst H., Geibler P. *Handbook of computer vision and applications*, volume 1, 2, 3 academic press. 1999.
  - [35] N. Montés, F.Sánchez, J.A.Garcia, A.Falco, J.Tornero, F.Chinesta. *Application of Artificial Vision in flow redirection during filling of Liquid Composite Molding processes.* AIP Conf. Proc. -- April 7, 2007 -- Volume 907, pp. 902-907